

# Structure–Property Correlations in the Platinum Oxide and Palladium Sulfide Bronzes with Columnar Chains of Square-Planar TX<sub>4</sub> Units (T = Pt, X = O; T = Pd, X = S)

Marie-Liesse Doublet,<sup>†</sup> Enric Canadell,<sup>\*,†</sup> and Myung-Hwan Whangbo<sup>\*,†</sup>

Contribution from the Laboratoire de Chimie Théorique, Université de Paris-Sud, 91405 Orsay, France, and Department of Chemistry, North Carolina State University, Raleigh, North Carolina 27695-8204

Received September 10, 1993. Revised Manuscript Received December 9, 1993<sup>⊙</sup>

**Abstract:** We carried out tight-binding electronic band structure calculations for the three representative types of ternary platinum oxides with columnar PtO<sub>4</sub> chains, NaPt<sub>3</sub>O<sub>4</sub>, CaPt<sub>2</sub>O<sub>4</sub>, and CdPt<sub>3</sub>O<sub>6</sub>, and for LaPd<sub>3</sub>S<sub>4</sub>, the sulfur analog of NaPt<sub>3</sub>O<sub>4</sub>. As far as the z<sup>2</sup> bands are concerned, the three orthogonal columnar PtO<sub>4</sub> chains of NaPt<sub>3</sub>O<sub>4</sub> are nearly independent, but NaPt<sub>3</sub>O<sub>4</sub> does not undergo a metal-to-insulator transition. This implies that the lattice of NaPt<sub>3</sub>O<sub>4</sub> is too stiff to accommodate a periodic lattice distortion associated with the partially filled z<sup>2</sup> bands. As far as the x<sup>2</sup> – y<sup>2</sup> bands are concerned, however, the three orthogonal columnar TX<sub>4</sub> chains of the MT<sub>3</sub>X<sub>4</sub> lattice (T = Pt, X = O; T = Pd, X = S) are not independent. Due to the through-bond σ interactions that occur between the columnar TX<sub>4</sub> chains, the partially-filled x<sup>2</sup> – y<sup>2</sup> bands are wide and possess 3D character. This explains why (RE)Pd<sub>3</sub>S<sub>4</sub> is metallic. Despite the dimerization in its columnar PtO<sub>4</sub> chains, CaPt<sub>2</sub>O<sub>4</sub> is metallic because the upper half of the z<sup>2</sup> band overlaps with other d-block bands. The dimerization of the columnar PtO<sub>4</sub> chains does not represent a charge density wave instability but is probably caused by the alternation of filled and unfilled square-prism sites along each chain. The very small band gap of CdPt<sub>3</sub>O<sub>6</sub> (0.04 eV) does not represent the energy separation between the z<sup>2</sup> and x<sup>2</sup> – y<sup>2</sup> bands but may originate from holes introduced into the z<sup>2</sup> band by nonstoichiometry and counterion disorder.

## Introduction

Some ternary platinum oxides<sup>1</sup> contain columnar PtO<sub>4</sub> chains, i.e., columnar stacks of parallel square-planar PtO<sub>4</sub> groups. There are three types of ternary platinum oxides with columnar PtO<sub>4</sub> chains. These chains run in three mutually orthogonal directions in the M<sub>3</sub>Pt<sub>3</sub>O<sub>4</sub> phase,<sup>2</sup> in two mutually orthogonal directions in the MPt<sub>2</sub>O<sub>4</sub> phase,<sup>3</sup> and only in one direction in the MPt<sub>3</sub>O<sub>6</sub> phase.<sup>4</sup> To a first approximation, the columnar PtO<sub>4</sub> chains of these oxides can be considered as independent of one another. Whether or not these oxides are metallic is commonly discussed in terms of the mixed-valence classification scheme given by Robin and Day<sup>5</sup> and the occupancy of the qualitative z<sup>2</sup> band expected for a columnar PtO<sub>4</sub> chain.<sup>6</sup> In general, one-dimensional (1D) metals are susceptible to a periodic lattice distortion that opens a band gap at the Fermi level, which is often referred to as a Peierls instability or a charge density wave (CDW) instability.<sup>7</sup> The typical example is a 1D chain with half-filled band, which

tends to undergo a dimerization thereby opening a band gap at the Fermi level. This provides an explanation for the occurrence of the Pt<sup>2+</sup>/Pt<sup>4+</sup> mixed-valence systems<sup>5</sup> and their nonmetallic properties.<sup>5,8</sup> Platinum chain systems with partially oxidized platinum ions, Pt<sup>(2+δ)+</sup>, possess partially empty z<sup>2</sup> bands<sup>6,9</sup> and hence are typically metals around room temperature.<sup>10</sup>

The platinum oxides with the columnar PtO<sub>4</sub> chains exhibit somewhat puzzling structural and physical properties. For example, the platinum oxidation state in NaPt<sub>3</sub>O<sub>4</sub> is +2.333, which suggests that its z<sup>2</sup> band (from the viewpoint of the chain with one metal atom per repeat unit) is one-sixth empty and hence the instability toward a hexamerization distortion. However, NaPt<sub>3</sub>O<sub>4</sub> shows a uniform Pt–Pt distance and is a metal with high conductivity. Thus, one might speculate if the three mutually orthogonal columnar PtO<sub>4</sub> chains interact to some extent to reduce the 1D character. In the CaPt<sub>2</sub>O<sub>4</sub> phase, the platinum oxidation state is +3, which suggests a half-filled z<sup>2</sup> band and hence a dimerization instability. Indeed, the columnar PtO<sub>4</sub> chains of CaPt<sub>2</sub>O<sub>4</sub> are dimerized (with Pt–Pt distances of 2.79 and 2.99 Å), but CaPt<sub>2</sub>O<sub>4</sub> is not semiconducting but metallic as if the dimerization is not caused by a CDW instability. The MPt<sub>3</sub>O<sub>6</sub> phase contains two types of chains, one columnar PtO<sub>4</sub> chain and two edge-sharing octahedral chains per formula unit (see Figure 8 and below for further discussion). With divalent

<sup>†</sup> Université de Paris-Sud.

<sup>†</sup> North Carolina State University.

<sup>⊙</sup> Abstract published in *Advance ACS Abstracts*, February 1, 1994.

(1) For a review, see: Schwartz, K. B.; Prewitt, C. T. *J. Phys. Chem. Solids* **1984**, *45*, 1.

(2) (a) Schwartz, K. B.; Parise, J. B.; Prewitt, C. T.; Shannon, R. D. *Acta Crystallogr. B* **1982**, *38*, 2109. (b) Schwartz, K. B.; Prewitt, C. T.; Shannon, R. D.; Corliss, L. M.; Hastings, J. M.; Chamberland, B. L. *Acta Crystallogr. B* **1982**, *38*, 363. (c) Shannon, R. D.; Gier, T. E.; Garcia, P. F.; Bierstedt, P. E.; Flippen, R. B.; Vega, A. J. *Inorg. Chem.* **1982**, *21*, 3372. (d) Cahen, D.; Ibers, J. A.; Wagner, J. B., Jr. *Inorg. Chem.* **1974**, *13*, 1377. (e) Cahen, D.; Ibers, J. A.; Shannon, R. D. *Inorg. Chem.* **1972**, *11*, 2311. (f) Waser, J.; McClanahan, E. D., Jr. *J. Chem. Phys.* **1951**, *19*, 413.

(3) Cahen, D.; Ibers, J. A.; Mueller, M. H. *Inorg. Chem.* **1974**, *13*, 110.

(4) (a) Hriljac, J. A.; Parise, J. B.; Kwei, G. H.; Schwartz, K. B. *J. Phys. Chem. Solids* **1991**, *52*, 1273. (b) Prewitt, C. T.; Schwartz, K. B.; Shannon, R. D. *Acta Crystallogr. C* **1983**, *39*, 519. (c) Schwartz, K. B.; Parise, J. B.; Prewitt, C. T.; Shannon, R. D. *Acta Crystallogr. B* **1983**, *39*, 217. (d) Schwartz, K. B.; Parise, J. B.; Prewitt, C. T. *Acta Crystallogr. B* **1983**, *39*, 525. (e) Schwartz, K. B.; Parise, J. B. *J. Phys. Chem. Solids* **1982**, *43*, 911.

(5) Robin, M.; Day, P. *Adv. Inorg. Chem. Radiochem.* **1967**, *10*, 247.

(6) For qualitative band structure descriptions of columnar platinum chain systems, see: (a) Krogmann, K. *Angew. Chem., Int. Ed. Engl.* **1969**, *8*, 35. (b) Miller, J. S.; Epstein, A. J. *Prog. Inorg. Chem.* **1976**, *20*, 1.

(7) For recent reviews, see: (a) *Electronic Properties of Inorganic Quasi-One-Dimensional Compounds*; Monceau, P., Ed.; Reidel: Dordrecht, The Netherlands, 1985; Parts I and II. (b) *Crystal Chemistry and Properties of Materials with Quasi-One-Dimensional Structures*; Rouxel, J., Ed.; Reidel: Dordrecht, The Netherlands, 1986. (c) *Structure Phase Transitions in Layered Transition Metal Compounds*; Motizuki, K., Ed.; Reidel: Dordrecht, The Netherlands, 1986. (d) *Low-Dimensional Electronic Properties of Molybdenum Bronzes and Oxides*; Schlenker, C., Ed.; Kluwer Academic Publ.: Dordrecht, The Netherlands, 1989. (e) Pouget, J. P. In *Semiconductors and Semimetals*; Conwell, E., Ed.; Academic Press: New York, 1988; Vol. 27, p 87.

(8) Whangbo, M.-H.; Foshee, M. J. *Inorg. Chem.* **1981**, *20*, 113.

(9) Whangbo, M.-H.; Hoffmann, R. *J. Am. Chem. Soc.* **1978**, *100*, 6093.

(10) Williams, J. M.; Schultz, A. J.; Underhill, A. E.; Carneiro, K. In *Extended Linear Chain Compounds*; Miller, J. S., Ed.; Plenum: New York, 1982; p 73.

cations  $M^{2+}$  and  $Pt^{4+}$  in the octahedral chains, the oxidation state of Pt in the columnar  $PtO_4$  chains of the  $MPt_3O_6$  phase is +2. This suggests a large band gap between the  $z^2$  and  $x^2 - y^2$  bands and hence a semiconducting property. Conductivity measurements show that the  $CdPt_3O_6$  phase is indeed a semiconductor, but its band gap is very small (i.e., 0.04 eV) compared with the expected energy gap between the  $x^2 - y^2$  and  $z^2$  bands of their columnar  $PtO_4$  chains (of the order of 1 eV). Finally we note that the sulfide bronzes  $(RE)Pd_3S_4$  ( $RE =$  rare earth) are isostructural with the platinum bronzes  $MPt_3O_4$  and are metallic as well.<sup>11</sup> The typical oxidation state of  $RE^{3+}$  implies that the  $z^2$  bands of the  $Pd_3S_4^{3-}$  lattice are completely filled, and an electron per  $Pd_3S_4$  formula unit is then left over to fill the  $x^2 - y^2$  bands of the  $Pd_3S_4^{3-}$  lattice. From the viewpoint of columnar  $PdS_4$  chains, the  $x^2 - y^2$  orbitals are  $\delta$  orbitals along the chain direction so that the  $x^2 - y^2$  band might be expected to be very narrow. Since electron localization is favorable in a system with a partially filled narrow band system,<sup>12</sup> it is apparently surprising that the sulfide bronzes  $(RE)Pd_3S_4$  are observed to be metallic. In order to examine these apparently puzzling observations, we carry out electronic band structure for the representative platinum oxides with the columnar  $PtO_4$  chains as well as the sulfide bronze  $LaPd_3S_4$  by employing the extended Hückel tight binding (EHTB) method.<sup>9,13</sup> The atomic orbital parameters employed in our EHTB calculations are listed in Table 1.

#### d-Block Bands of an Ideal Columnar $PtO_4$ Chain

To facilitate our discussion of the electronic band structures of the platinum oxides studied in the present work, it is convenient to first consider the d-block bands of an ideal columnar  $PtO_4$  chain 1 constructed with  $Pt-O = 2.01 \text{ \AA}$  and  $Pt-Pt = 2.84 \text{ \AA}$ .

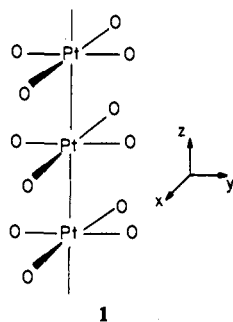


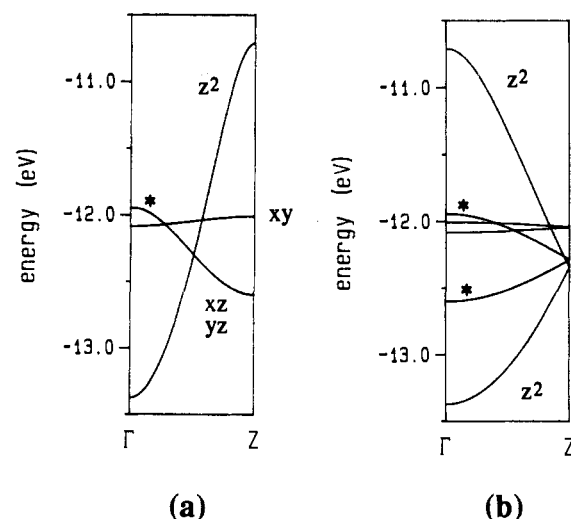
Figure 1a shows the dispersion relations of the d-block bands of this chain calculated with one  $PtO_4$  unit per repeat unit cell, and Figure 1b shows the corresponding ones calculated with two  $PtO_4$  units per repeat unit cell. Figure 1 shows that the  $xz$ ,  $yz$ , and  $xy$  bands occur in the middle portion of the  $z^2$  band. Along the chain, the  $z^2$  orbitals make  $\sigma$  interactions, the  $xz/yz$  orbitals  $\pi$  interactions, and the  $xy$  orbitals  $\delta$  interactions. Consequently, the extent of band dispersion increases in the order  $xy < xz, yz < z^2$ . (In our discussion of the d-block bands of the platinum oxide bronzes, the  $x^2 - y^2$  bands lie above the  $z^2$  bands and are not considered unless stated otherwise.)

Figure 1b shows that when the unit cell size is doubled, each band is doubly folded. Note that the  $xy$  band overlaps with the upper half of the folded  $z^2$  band, which plays an important role in determining the physical properties of  $CaPt_2O_4$  (see below). Another important aspect of the band folding concerns an electron counting with band filling. For the columnar  $PtO_4$  chain with  $Pt^{2.333+}$  in  $NaPt_3O_4$ , for example, the  $z^2$  band is one-sixth empty

**Table 1.** The Exponents  $\zeta_l$  and the Valence Shell Ionization Potentials  $H_{ll}$  for Slater-Type Atomic Orbitals  $\chi_l^{a,b}$

atom	$\chi_l$	$\zeta_l$	$\zeta_l'$	$H_{ll}$ (eV)
O	2s	2.275		-32.3
O	2p	2.275		-14.8
S	3s	1.817		-20.0
S	3p	1.817		-13.3
Pd	5s	2.19		-9.20
Pd	5p	2.15		-5.30
Pd	4d	5.98 (0.5264)	2.613 (0.6372)	-12.9
La	6s	2.14		-7.67
La	6p	2.08		-5.01
La	5d	3.78 (0.7766)	1.38 (0.4587)	-8.21
Pt	6s	2.554		-9.08
Pt	6p	2.554		-5.47
Pt	5d	6.013 (0.6334)	2.696 (0.5513)	-12.6

<sup>a</sup>  $H_{ll}$ 's are the diagonal matrix elements  $\langle \chi_l | H^{\text{eff}} | \chi_l \rangle$ , where  $H^{\text{eff}}$  is the effective Hamiltonian. In our calculations of the off-diagonal matrix elements  $H_{ij} = \langle \chi_i | H^{\text{eff}} | \chi_j \rangle$ , the weighted formula was used.<sup>13b</sup> <sup>b</sup> The 5d orbitals of Pd, La, and Pt are given as a linear combination of two different Slater-type orbitals, and each is followed by the weighting coefficient in parentheses.



**Figure 1.** Dispersion relations of the d-block bands calculated for an ideal columnar  $PtO_4$  chain 1 (with  $Pt-O = 2.01 \text{ \AA}$  and  $Pt-Pt = 2.84 \text{ \AA}$ ): (a) with one  $PtO_4$  unit per repeat unit cell and (b) with two  $PtO_4$  units per repeat unit cell.  $\Gamma = 0$ .  $Z = \pi/c$  in (a) and  $Z = \pi/2c$  in (b), where  $c$  is the  $Pt-Pt$  repeat distance. A doubly degenerate band is labeled with an asterisk.

in the representation of one metal per repeat unit (e.g., Figure 1a). In the doubled unit cell representation (e.g., Figure 1b), the  $z^2$  band is doubly folded so that the lower half is completely filled and the upper half is one-third empty. This consideration applies to the case of  $NaPt_3O_4$  examined in the next section.

#### $MPt_3O_4$ Phase

As a representative example of this phase, we consider  $NaPt_3O_4$ , for which the platinum oxidation state is +2.333. As shown in Figure 2, this phase has three mutually orthogonal columnar  $PtO_4$  chains. Each oxygen atom belongs to three orthogonal chains, and each  $Na^+$  ion is at the center of a square prism of oxygen atoms. Along each chain direction, there occur square prism sites between every two  $Pt-Pt$  bonds. However, the  $Na^+$  ions are found only at every second square-prism site, and this occurs in three orthogonal directions in such a way that all  $Pt-Pt$  bonds have identical environments. The unit cell of  $NaPt_3O_4$  has two formula units  $(NaPt_3O_4)_2$ , and each columnar  $PtO_4$  chain has two metal atoms per repeat unit. Therefore, the  $z^2$  band of each chain will be doubly folded as in Figure 1b. In the three-dimensional (3D) lattice, there are three mutually orthogonal chain directions. Provided that there are no interactions among the

(11) Kesler, D. A.; Ibers, J. A. *Inorg. Chem.* 1983, 22, 3366.

(12) (a) Mott, N. F. *Metal-Insulator Transitions*; Barnes and Noble: New York, 1977. (b) Brandow, B. H. *Adv. Phys.* 1977, 26, 651. (c) Whangbo, M.-H. *J. Chem. Phys.* 1979, 70, 4963.

(13) (a) Hoffmann, R. *J. Chem. Phys.* 1963, 39, 1397. (b) Ammeter, J. H.; Bürgi, H.-B.; Thibault, J.; Hoffmann, R. *J. Am. Chem. Soc.* 1978, 100, 3686.

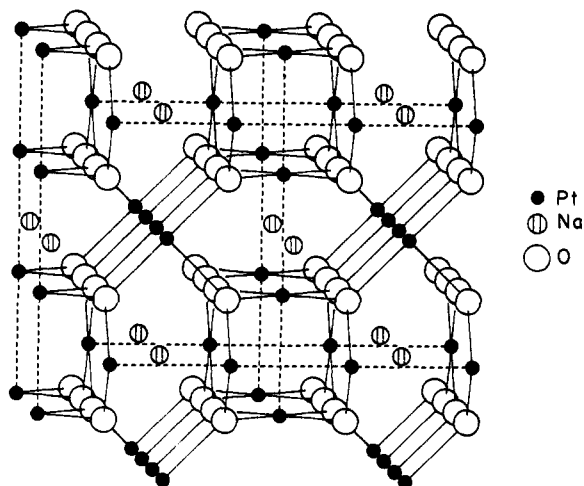


Figure 2. Perspective view of the crystal structure of  $\text{NaPt}_3\text{O}_4$ , where Pt, Na, and O atoms are represented by small filled, medium hatched, and large open circles, respectively. The Pt-Pt contacts of the columnar  $\text{PtO}_4$  chains are shown by dashed lines.

three orthogonal chains, the  $z^2$  band of each chain is dispersive along its own chain direction but flat in other chain directions. Thus, the  $z^2$  band dispersion relations expected for such a 3D lattice along  $\Gamma \rightarrow X \rightarrow M \rightarrow R$  (for the definition of  $\Gamma$ ,  $X$ ,  $M$ , and  $R$ , see the first Brillouin zone 2) are given as sketched in 3, where the bands labeled with an asterisk are doubly degenerate.

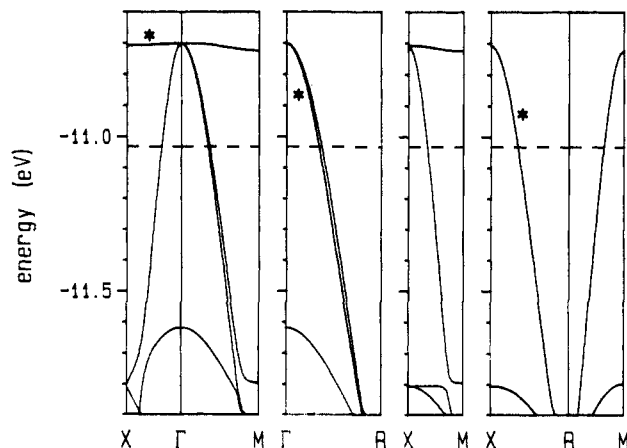
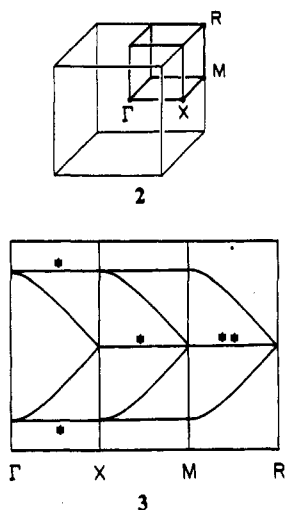


Figure 3. Dispersion relations of the top portion of the occupied d-block bands calculated for  $\text{NaPt}_3\text{O}_4$ , where the dashed line refers to the Fermi level.  $\Gamma = (0, 0, 0)$ ,  $X = (a^*/2, 0, 0)$ ,  $M = (a^*/2, b^*/2, 0)$ , and  $R = (a^*/2, b^*/2, c^*/2)$ . A doubly degenerate band is labeled with an asterisk.

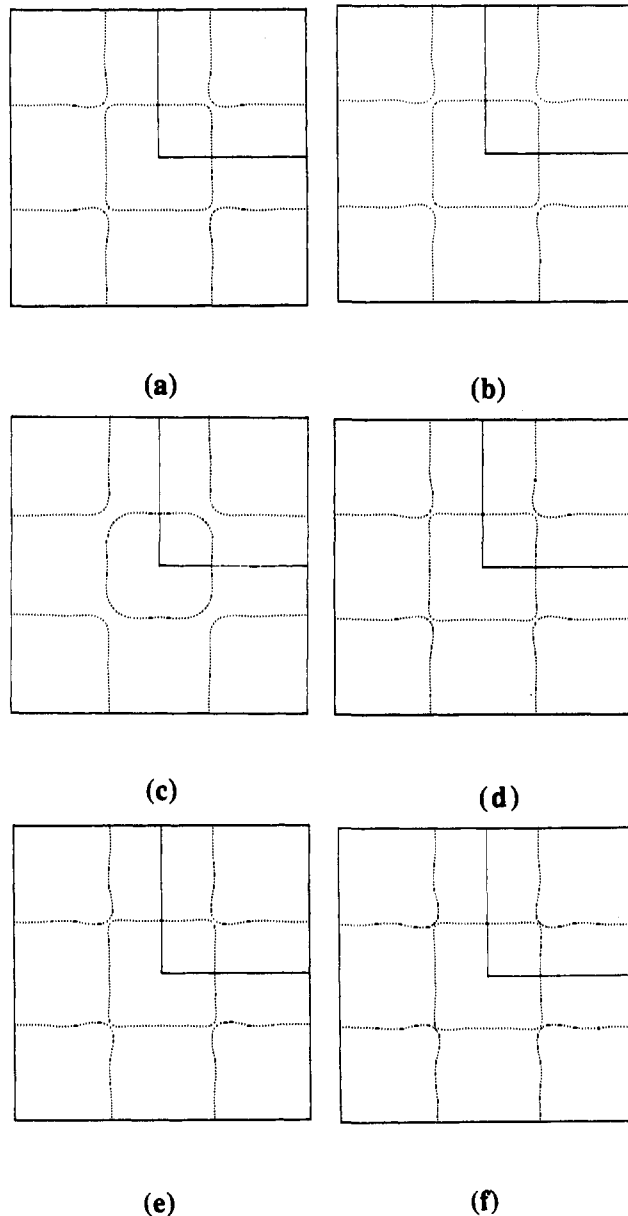


Figure 4. Cross sections, perpendicular to the  $\Gamma \rightarrow Z$  direction, of the Fermi surface calculated for  $\text{NaPt}_3\text{O}_4$  at the  $c^*$  height of (a) 0, (b)  $0.1c^*$ , (c)  $0.2c^*$ , (d)  $0.3c^*$ , (e)  $0.4c^*$ , and (f)  $0.5c^*$ .

The d-block bands calculated for the 3D lattice of  $\text{NaPt}_3\text{O}_4$  are shown in Figure 3, where the bands labeled with an asterisk are doubly degenerate, and the dashed line refers to the Fermi level. For simplicity only the top portion of the highest occupied bands is shown. The bands at the top portion of Figure 3 are the  $z^2$  bands, which correspond to the upper half of the schematic bands in 3. The bands of the 3D  $\text{NaPt}_3\text{O}_4$  lattice exhibit characteristics quite similar to those expected for the 3D lattice of three orthogonal, noninteracting chains. This suggests that the three orthogonal chains are nearly independent as far as the  $z^2$  bands are concerned.

Figure 4 shows the Fermi surface calculated for the  $\text{NaPt}_3\text{O}_4$  lattice as a series of six cross-section views perpendicular to the  $\Gamma \rightarrow Z$  direction. From the conceptual viewpoint of the hidden Fermi surface,<sup>14</sup> it is easy to recognize a pair of nearly parallel planes perpendicular to  $\Gamma \rightarrow X$  and another pair perpendicular

(14) (a) Whangbo, M.-M.; Canadell, E.; Foury, P.; Pouget, J. P. *Science*, 1991, 252, 96. (b) Canadell, E.; Whangbo, M.-H. *Chem. Rev.* 1991, 91, 965. (c) Whangbo, M.-H.; Canadell, E. *J. Am. Chem. Soc.* 1992, 114, 9587. (d) Whangbo, M.-H.; Ren, J.; Liang, W.; Canadell, E.; Pouget, J.-P.; Ravy, S.; Williams, J. M.; Beno, M. A. *Inorg. Chem.* 1992, 31, 4169.

to  $\Gamma \rightarrow Y$ . These are the 1D Fermi surfaces for the chains running along the  $a$  and  $b$  directions, respectively. (The separation between

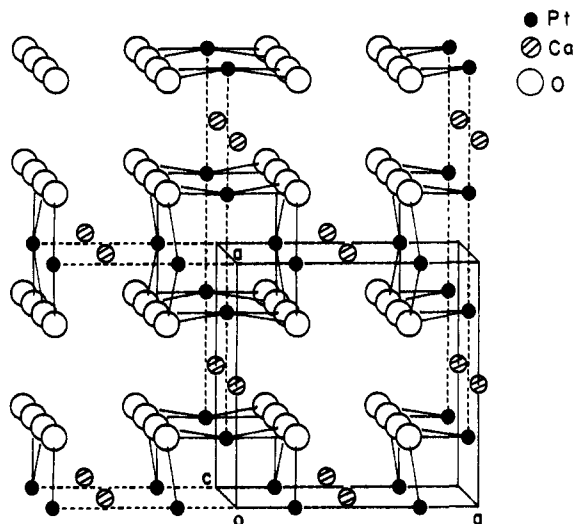


**Figure 5.** Perspective view of the crystal structure of  $\text{CaPt}_2\text{O}_4$ , where Pt, Ca, and O atoms are represented by small filled, medium hatched, and large open circles, respectively. The Pt-Pt contacts of the columnar  $\text{PtO}_4$  chains are shown by dashed lines.

the parallel planes, e.g.,  $a^*/3$  along  $\Gamma \rightarrow X$  and  $b^*/3$  along  $\Gamma \rightarrow Y$ , shows that each  $z^2$  band is one-third empty, which corresponds to the platinum oxidation state  $\text{Pt}^{2.333+}$ .) Though not shown in Figure 4, there are two more nearly parallel planes perpendicular to  $\Gamma \rightarrow Z$  representing the 1D Fermi surface for the chains running along the  $c$  direction. Consequently, in terms of the calculated Fermi surfaces as well, we reach the same conclusion that the three orthogonal chains of the  $\text{NaPt}_3\text{O}_4$  lattice are nearly independent as far as the  $z^2$  bands are concerned.

Thus, the interchain interactions in  $\text{NaPt}_3\text{O}_4$  are too weak to destroy the 1D character of the Fermi surface and cannot be responsible for the absence of a metal-to-insulator transition in  $\text{NaPt}_3\text{O}_4$ . It is important to note that the presence of the 1D Fermi surface is neither sufficient nor necessary for the observation of periodic lattice distortions in solids. For example,  $\text{Na}_3\text{Cu}_4\text{S}_4$  is a strongly 1D metal<sup>15</sup> but does not show any CDW instability down to  $\sim 10$  K.<sup>16</sup> Probably, the phonon coupling with the electrons at the Fermi level induces a strong lattice strain.<sup>15</sup> By analogy, one might suggest that the 3D lattice is too stiff to accommodate a periodic lattice distortion associated with the partially filled  $z^2$  bands. This is consistent with the observation that the electrical conductivity of  $\text{NaPt}_3\text{O}_4$  is very high, because the latter implies a weak phonon scattering and hence a stiff lattice. This point is discussed further in the next section.

### $\text{CaPt}_2\text{O}_4$ Phase

Figure 5 shows the crystal structure of  $\text{CaPt}_2\text{O}_4$ , in which the columnar  $\text{PtO}_4$  chains run in two orthogonal directions, and a metal atom dimerization ( $\text{Pt-Pt} = 2.79, 2.99 \text{ \AA}$ ) is present along each chain direction. As in the case of  $\text{NaPt}_3\text{O}_4$ , along each chain direction of  $\text{CaPt}_2\text{O}_4$ , there occur square prism sites between every two Pt-Pt bonds, and the  $\text{Ca}^{2+}$  ions are found only at every second square-prism site. The latter occurs only in two directions in  $\text{CaPt}_2\text{O}_4$ , so that there occur two different Pt-Pt bond environments alternating along the chain direction (even if all the Pt-Pt bonds were identical in length). The platinum oxidation state is +3, so that, had the columnar  $\text{PtO}_4$  chain a uniform Pt-Pt distance, the  $z^2$  band would be half filled. The dimerization will split the half-filled  $z^2$  band into two, thereby leaving the lower subbands completely filled and upper subbands completely empty and predicting an insulating property. Figure 6 shows the d-block bands calculated for a single columnar  $\text{PtO}_4$  chain taken

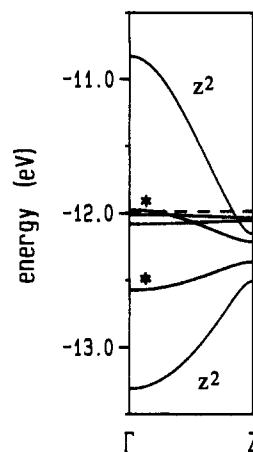


**Figure 6.** Dispersion relations of the d-block bands calculated for a single columnar  $\text{PtO}_4$  chain of  $\text{CaPt}_2\text{O}_4$ , where the dashed line refers to the Fermi level corresponding to the platinum oxidation state of  $\text{Pt}^{3+}$ .  $\Gamma = 0$  and  $Z = c^*/2$ . A doubly degenerate band is labeled with an asterisk.

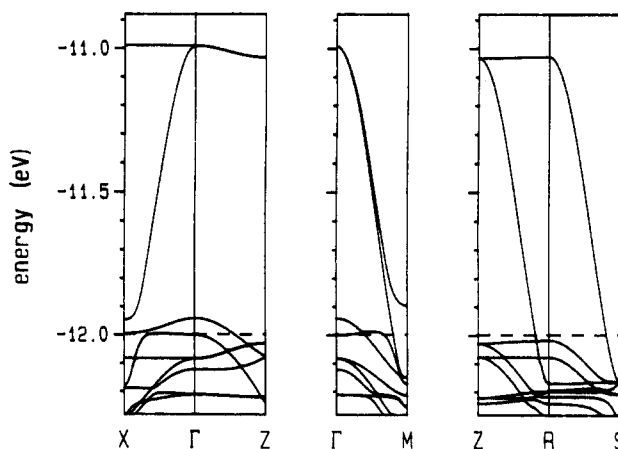


**Figure 7.** Dispersion relations of the top portion of the occupied d-block bands calculated for  $\text{CaPt}_2\text{O}_4$ , where the dashed line refers to the Fermi level.  $\Gamma = (0, 0, 0)$ ,  $X = (a^*/2, 0, 0)$ ,  $M = (a^*/2, b^*/2, 0)$ ,  $R = (a^*/2, 0, c^*/2)$ , and  $S = (a^*/2, b^*/2, c^*/2)$ .

from  $\text{CaPt}_2\text{O}_4$ . With respect to the case of Figure 1b, each band of Figure 6 is split into two, as expected. Note that the upper  $z^2$  band overlaps with the upper  $xz, yz$  bands and with the upper and lower  $xy$  bands. Because of this overlap there is no band gap for the columnar  $\text{PtO}_4$  chains with  $\text{Pt}^{3+}$  ions, so that the chain is expected to be metallic even with the dimerization. The same conclusion is reached from the electronic band structure calculations for the 3D lattice of  $\text{CaPt}_2\text{O}_4$ , which is summarized in Figure 7.

The energy gain for a CDW instability occurs only when the upper band raised by the emerging band gap is unfilled. Notice from Figures 6 and 7 that the Fermi level occurs at a position well above the band gap of the split  $z^2$  bands. Consequently, the dimerization of the columnar  $\text{PtO}_4$  chains present in  $\text{CaPt}_2\text{O}_4$  is not driven by a CDW instability. As already discussed in Figure 5, the crystal structure of  $\text{CaPt}_2\text{O}_4$  possesses two different Pt-Pt bond environments alternating along the chain direction even if all the Pt-Pt bonds were identical in length. Therefore, the Pt-Pt...Pt bond alternation should be a consequence of the crystal packing forces dictated by the two nonequivalent environments along each chain.

In the case of the  $\text{NaPt}_3\text{O}_4$  system, all the Pt-Pt bond environments are identical so that the crystal packing forces lead to the  $\text{PtO}_4$  chains with uniform Pt-Pt bonds. Due to these crystal packing forces, it may be difficult to distort the  $\text{PtO}_4$  chains of the  $\text{NaPt}_3\text{O}_4$  by a CDW mechanism unless the electronic energy gain due to the CDW can overcome the strain presented by the crystal packing forces. In general, the electronic energy gain by

(15) Whangbo, M.-M.; Canadell, E. *Inorg. Chem.* 1990, 29, 1395.

(16) Pepilnski, Z.; Brown, D. B.; Watt, T.; Hatfield, W. E.; Day, P. *Inorg. Chem.* 1982, 21, 1752.

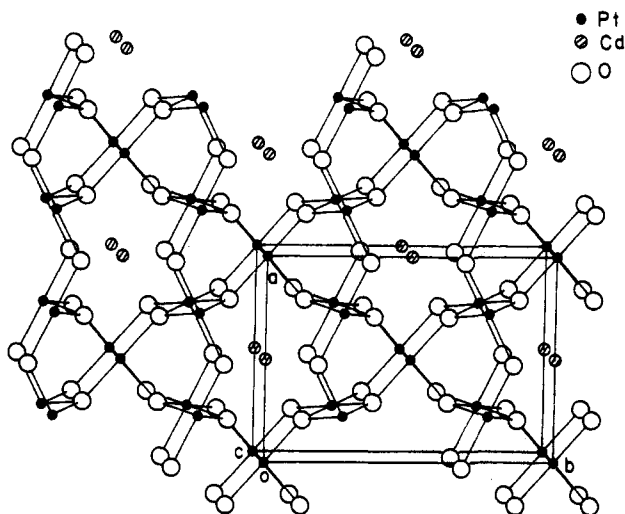


Figure 8. Perspective view of the crystal structure of  $\text{CdPt}_3\text{O}_6$ , where Pt, Cd, and O atoms are represented by small filled, medium hatched, and large open circles, respectively.

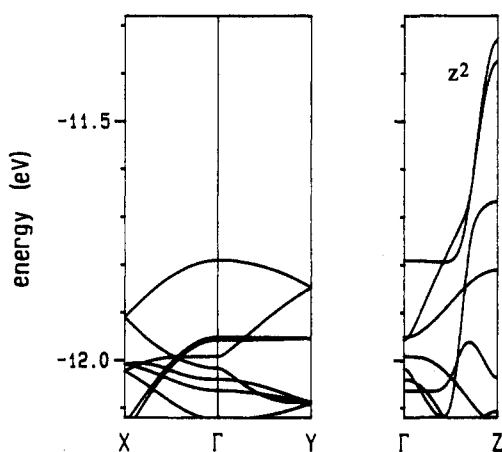


Figure 9. Dispersion relations of the top portion of the occupied d-block bands calculated for  $\text{CdPt}_3\text{O}_6$ .  $\Gamma = (0, 0, 0)$ ,  $X = (a^*/2, 0, 0)$ ,  $Y = (0, b^*/2, 0)$ ,  $Z = (0, 0, c^*/2)$ .

a CDW mechanism is strongest for a system with a half-filled band, and it decreases when the band occupancy deviates from the half-filled situation.<sup>17</sup> Simply speaking, the  $\text{NaPt}_3\text{O}_4$  system has three one-sixth-empty 1D bands (from the viewpoint of one Pt atom per unit cell in a chain), so that the electronic energy gain resulting from the associated CDW instability is not expected to be large. This plus the aforementioned tendency of the packing forces may be the reason why the  $\text{NaPt}_3\text{O}_4$  system shows no distortion in the  $\text{PtO}_4$  chains.

### $\text{MPt}_3\text{O}_6$ Phase

Figure 8 shows the crystal structure of  $\text{CdPt}_3\text{O}_6$ , which consists of two types of chains. One is the columnar  $\text{PtO}_4$  chains running along the  $c$ -axis direction. The other is the octahedral  $\text{PtO}_4$  chains, made up of  $\text{PtO}_6$  octahedra by sharing their edges, running along the  $c$ -axis direction. (The edge-sharing octahedral chains share their corners along the  $a$  direction to form a layer.) A unit cell contains two columnar  $\text{PtO}_4$  chains and two octahedral  $\text{PtO}_4$  chains, and each columnar  $\text{PtO}_4$  chain has one Pt atom per repeat unit. The platinum oxidation state at the octahedral coordination site is regarded as +4, which provides six electrons just to fill the  $t_{2g}$  levels. With the oxidation state of  $\text{Cd}^{2+}$ , the platinum oxidation state in the columnar  $\text{PtO}_4$  chains is +2.

Figure 9 shows the top portion of the occupied bands calculated for  $\text{CdPt}_3\text{O}_6$ . The two bands at the top (see the dispersion along

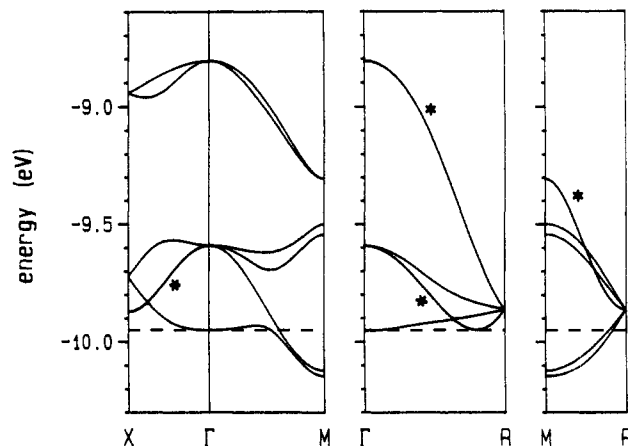


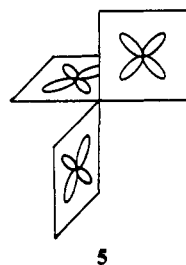
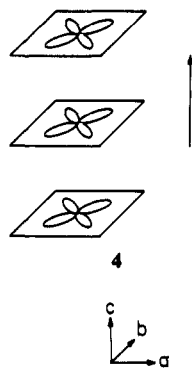
Figure 10. Dispersion relations of the  $x^2-y^2$  bands calculated for  $\text{LaPd}_3\text{S}_4$ , where the dashed line refers to the Fermi level.  $\Gamma = (0, 0, 0)$ ,  $X = (a^*/2, 0, 0)$ ,  $M = (a^*/2, b^*/2, 0)$ , and  $R = (a^*/2, b^*/2, c^*/2)$ . A doubly degenerate band is labeled with an asterisk.

$\Gamma \rightarrow Z$ ) are the  $z^2$  bands of the columnar  $\text{PtO}_4$  chains, and they overlap strongly with many bands, most of which are associated with the octahedral chains. Although not shown for simplicity in Figure 9, there is a band gap of about 1.2 eV, whereas according to the conductivity measurements,  $\text{MPt}_3\text{O}_6$  has a very small band gap (i.e., 0.04–0.07 eV). This apparent contradiction can be explained in terms of the nonstoichiometry of chemical composition such as M deficiency that introduces holes in the  $z^2$  band. In fact, neutron powder diffraction studies show that  $\text{MPt}_3\text{O}_6$  is an approximate formula. Compositions with M = Mn or Co are found to contain vacancies in the square-prism sites and some  $\text{M}^{2+}$  ions in the octahedral  $\text{Pt}^{4+}$  sites. This nonstoichiometry and counterion disorder lead to partial oxidation of the columnar stacks and enhance the conductivity. However, the nonstoichiometry and counterion disorder also create random potentials in the lattice. Thus, when the concentration of holes is not high, they may become weakly trapped so that their movement is activated. This might explain the small activation energy observed for  $\text{MPt}_3\text{O}_6$ .

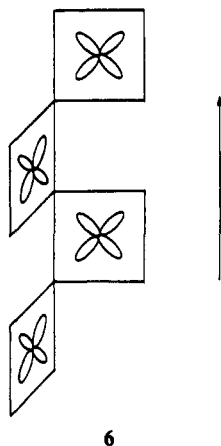
### Sulfide Bronze $(\text{RE})\text{Pd}_3\text{S}_4$ (RE = Rare Earth)

As already mentioned, the sulfide bronzes  $(\text{RE})\text{Pd}_3\text{S}_4$  are isostructural with the platinum bronzes  $\text{MPt}_3\text{O}_4$ <sup>11</sup> so that the unit cell of  $(\text{RE})\text{Pd}_3\text{S}_4$  has two formula units,  $[(\text{RE})\text{Pd}_3\text{S}_4]_2$ . With the electron counting  $(\text{Pd}_3\text{S}_4^{3-})_2$  per unit cell, there are two electrons to fill the  $x^2-y^2$  bands of the 3D lattice of  $\text{LaPd}_3\text{S}_4$ . The dispersion relations of the  $x^2-y^2$  bands calculated for the 3D lattice of  $\text{LaPd}_3\text{S}_4$  are presented in Figure 10, where the bands labeled with asterisks are doubly degenerate, and the dashed line refers to the Fermi level. Note that the  $x^2-y^2$  bands are substantially dispersive, in agreement with the observed metallic character of the sulfide bronzes. In addition, the bottom two partially filled  $x^2-y^2$  bands are dispersive in all three directions of the lattice, so that the sulfide bronzes  $(\text{RE})\text{Pd}_3\text{S}_4$  are predicted to be genuine 3D metals. If we adopt the viewpoint that the three columnar  $\text{PtO}_4$  chains of  $\text{MPt}_3\text{O}_4$  are practically independent, it is expected that the  $x^2-y^2$  bands of  $(\text{RE})\text{Pd}_3\text{S}_4$  are flat because, in each  $\text{PdS}_4$  columnar chain, the  $x^2-y^2$  orbitals are  $\delta$  orbitals along the chain direction (see 4). Though not shown earlier, the  $x^2-y^2$  bands calculated for  $\text{NaPt}_3\text{O}_4$  are also wide.

We now discuss why the  $x^2-y^2$  bands of the  $\text{MT}_3\text{X}_4$  (T = Pt, X = O; T = Pd, X = S) systems are dispersive. Each X atom of the  $\text{MT}_3\text{X}_4$  lattice belongs to three mutually orthogonal square-planar  $\text{TX}_4$  units (Figure 2) so that, as illustrated in 5, the " $x^2-y^2$ " orbitals in the three mutually orthogonal planes can interact through the T-X-T bridges. The through-bond  $\sigma$  interactions via these metal-ligand-metal bridges can lead to strong interactions. For instance, in the columnar  $\text{TX}_4$  chain along the  $z$



direction (4), the through-space overlap between the square-planar  $\text{TX}_4$  units along the chain is weak because the  $x^2 - y^2$  orbitals make  $\delta$  interactions. However, as illustrated in 6, strong



interactions along the  $z$  direction occur via the through-bond  $\sigma$

interactions of the square-planar  $\text{TX}_4$  units of the chains running along the  $x$  and  $y$  directions. In a similar manner, strong interactions along the  $x$  direction ( $y$  direction) occur via the through-bond  $\sigma$  interactions of the square-planar  $\text{TX}_4$  units of the chains running along the  $y$  and  $z$  directions (the  $x$  and  $z$  directions). Consequently, the resulting  $x^2 - y^2$  bands of the  $\text{MT}_3\text{X}_4$  lattice have genuine 3D character, namely, they are not a superposition of the 1D bands of the three mutually orthogonal chains as found for the  $z^2$  bands. (Although not shown, this point was confirmed by calculating the Fermi surfaces of the  $x^2 - y^2$  bands.) It is not the through-space interactions within each individual  $\text{PdS}_4$  columnar chains but the through-bond interactions between the columnar chains that are responsible for the 3D metallic character of the  $(\text{RE})\text{Pd}_3\text{S}_4$ .

#### Concluding Remarks

Our study shows that the three orthogonal chains of the  $\text{NaPt}_3\text{O}_4$  lattice are nearly independent, as far as the  $z^2$  bands are concerned. Nevertheless, a metal-to-insulator transition is absent in  $\text{NaPt}_3\text{O}_4$ . This implies that the 3D lattice is too stiff to accommodate a periodic lattice distortion associated with the partially filled  $z^2$  bands. However, the three orthogonal  $\text{TX}_4$  columnar chains of the  $\text{MT}_3\text{X}_4$  lattice ( $\text{T} = \text{Pt}$ ,  $\text{X} = \text{O}$ ;  $\text{T} = \text{Pd}$ ,  $\text{X} = \text{S}$ ) are not independent, as far as the  $x^2 - y^2$  bands are concerned. The  $x^2 - y^2$  bands are wide and possess 3D character due to the through-bond  $\sigma$  interactions that occur between the columnar  $\text{TX}_4$  chains. The columnar  $\text{PtO}_4$  chains of  $\text{CaPt}_2\text{O}_4$  contain  $\text{Pt}^{3+}$  ions and exhibit a metal atom dimerization. Nevertheless,  $\text{CaPt}_2\text{O}_4$  is metallic because the upper  $xz$ ,  $yz$  bands and the  $xy$  bands overlap with the upper  $z^2$  band. The dimerization of the columnar  $\text{PtO}_4$  chains in  $\text{CaPt}_2\text{O}_4$  cannot be caused by a CDW instability but most likely by the occurrence of  $\text{Ca}^{2+}$  ions at every second square-prism site along each chain. The electronic band structure of  $\text{MPt}_3\text{O}_6$  shows a large band gap in contrast to the very small activation energy experimentally observed. Nonstoichiometry and counterion disorder enhance the conductivity because of the partial oxidation of the columnar stacks they induce. However, they also induce random potentials which will trap the holes at low concentration thereby making their movement weakly activated.

**Acknowledgment.** This work was supported by the U.S. Department of Energy, Office of Basic Sciences, Division of Materials Sciences, under Grant No. DE-FG05-86ER45259, by NATO, under Grant No. CRG 910129, Scientific Affairs Division, and by Centre National de la Recherche Scientifique, France.